

Redox Regulation of CLIC1 by Cysteine Residues Associated with the Putative Channel Pore

Harpreet Singh and Richard H. Ashley

Biomedical Sciences, University of Edinburgh Medical School, Edinburgh, United Kingdom

ABSTRACT Chloride intracellular channels (CLICs) are putative pore-forming glutathione-S-transferase homologs that are thought to insert into cell membranes directly from the cytosol. We incorporated soluble, recombinant human CLIC1 into planar lipid bilayers to investigate the associated ion channels, and noted that channel assembly (unlike membrane insertion) required a specific lipid mixture. The channels formed by reduced CLIC1 were similar to those previously recorded from cells and “tip-dip” bilayers, and specific anti-CLIC1 antibodies inhibited them. However, the amplitudes of the filtered single-channel currents were strictly regulated by the redox potential on the “extracellular” (or “luminal”) side of the membrane, with minimal currents under strongly oxidizing conditions. We carried out covalent functional modification and site-directed mutagenesis of this controversial ion channel to test the idea that cysteine 24 is a critical redox-sensitive residue located on the extracellular (or luminal) side of membrane CLIC1 subunits, in a cysteine-proline motif close to the putative channel pore. Our findings support a simple structural hypothesis to explain how CLIC1 oligomers form pores in membranes, and suggest that native channels may be regulated by a novel mechanism involving the formation and reduction of intersubunit disulphide bonds.

INTRODUCTION

The pore-forming subunits of well-established eukaryotic ion channels are processed in the secretory pathway as conventional membrane proteins. In contrast, chloride intracellular channel (CLIC) proteins, including the putative anion channels CLIC1 (1) and CLIC4 (p64H1) (2), are synthesized without a leader sequence, and appear to insert into cell membranes directly, by a mechanism yet to be elucidated. Although CLIC proteins are members of the glutathione-S-transferase (GST) superfamily (3,4), other GST proteins, including omega GSTs (their closest structural relatives), do not share this unusual “autoinserting” ability (5). If CLICs prove to be biologically relevant ion channels, their remarkable properties will present a substantial challenge to our current understanding of membrane protein biogenesis and ion channel regulation (6).

Once inserted from the cytosol, CLIC1 and CLIC4 monomers span the cell (or organelle) membrane completely, with an external (or intraluminal) N-terminus and an odd number of transmembrane domains (TMDs), as demonstrated by protease digestion experiments and terminus-directed antibodies (2,7,8). Although the membrane forms of recombinant CLIC1 and CLIC4 are both associated with novel ion channel activity (8,9), these channels could be an artifact of artificial overexpression. The cellular proteins exist almost entirely in their soluble, cytosolic form (see, e.g., Suginta et al. (10)), and endogenous CLIC channels have been hard to detect. However, native CLICs appear to be more likely to form ion channels under specific conditions. For example, channel

activity is promoted when nucleoplasmic CLIC1 is liberated during cell division (9), and the probability of recording CLIC1-like channels from microglia increases significantly after exposure to Alzheimer’s A β peptide (11).

CLIC1 has been shown to be a pore-forming protein *in vitro*, but single-channel recordings have been inconsistent. Recombinant CLIC1 channels reconstituted by “tip-dipping” (12) proved to be similar to those recorded from cells, but CLIC1 channels reconstituted in planar bilayers (13,14) had much larger amplitudes under similar ionic conditions. It was speculated (12) that CLIC1 could form channel “aggregates”, with larger overall conductances, under certain conditions. Reminiscent of this behavior, patch-clamped CLIC4 channels had a unit conductance of ~ 1 pS (8), compared to novel unit currents of 10–50 pS when brain microsomes containing the recombinant protein were reconstituted in bilayers (2). Although this might represent channel “aggregation” in microsomes, an alternative explanation is that CLIC4 can regulate other cellular channels, as demonstrated recently for CLIC2 (15). CLICs might also form channel complexes involving different CLIC isoforms, or other unidentified proteins.

Experiments involving Cl[−] efflux through CLIC1 incorporated into small unilamellar liposomes (e.g., Tulk et al. (14) and Littler et al. (16)) have also been difficult to interpret. Most of the entrapped Cl[−] was only released by detergents, suggesting that very few liposomes contained functional channels, and efflux was exceptionally prolonged, extending over tens of seconds or several minutes, even with an inside negative membrane potential. Under these conditions, small vesicles containing just a single active channel should empty within a few milliseconds (17). We speculated that some of these inconsistencies might be related to the bilayer lipid composition, and began our present study by surveying the

Submitted August 15, 2005, and accepted for publication November 16, 2005.

Address reprint requests to Richard H. Ashley, Biomedical Sciences, University of Edinburgh Medical School, Edinburgh EH8 9XD, UK. E-mail: richard.ashley@ed.ac.uk.

© 2006 by the Biophysical Society

0006-3495/06/03/1628/11 \$2.00

doi: 10.1529/biophysj.105.072678

effects of membrane lipids on protein insertion and channel formation. Finally, another notable feature of CLIC1, CLIC4, and other CLIC proteins is the presence of several cysteine residues (like other GST family members), making them potentially susceptible to intrachain or intersubunit disulphide bond formation, or both. Indeed, membrane CLIC1 has been reported to form channels after the protein is first oxidized by H_2O_2 to produce an intrasubunit disulphide bond (16).

In this article, we describe the lipid-dependent reconstitution of CLIC1, analyze its single-channel conductance and selectivity, and identify specific, functionally important, redox-sensitive cysteine residues close to the extracellular (or luminal) side of the channel pore. To our knowledge, this is the first structure/function study of this novel class of putative ion channel, and it leads to a readily testable hypothesis to explain how cellular CLIC1 channels may be regulated in vivo.

MATERIALS AND METHODS

Expression and purification of CLIC1

Human *CLIC1* (cDNA clone MGC:74817 IMAGE:5585323, MRC gene-service, Cambridge, UK) was inserted into pHis8, a modified pET vector encoding an N-terminal octa-His tag and a thrombin cleavage site (18). The codon for cysteine 24 was altered to alanine by the "QuikChange" polymerase chain reaction method. Rat *CLIC4* cDNA (2) was also cloned into the same vector, and all the inserts were verified by sequencing (MWG Biotech, Ebersberg, Germany). Soluble octa-His tagged fusion proteins were expressed in *Escherichia coli* BL21 (DE3) cells and purified from cell lysates by Ni^{2+} -NTA affinity chromatography. Nonspecifically bound proteins were removed by extensive washing in 20 mM imidazole, and the tagged CLIC proteins were eluted by 150 mM imidazole in 150 mM NaCl containing 20 mM Tris-HCl (pH 8.0). All the solutions contained a stoichiometric excess of dithiothreitol (DTT). Enzymatic cleavage of the His tag left eight linker residues (sequence: GGLVPRGS) before the initiating methionine. The thrombin was removed by adding benzamidine Sepharose beads during dialysis to eliminate the imidazole, and fresh Ni-NTA beads were added to remove the cleaved His tags and any uncleaved protein. Some protein samples were also subjected to size-exclusion chromatography, but this step was not essential for subsequent experiments. The yield of CLIC1 was 4.4 ± 0.75 mg/l culture medium (mean \pm SD, $n = 7$), and protein aliquots were stored for up to 3 months at -70°C in buffer containing 5 mM DTT. Note that all the proteins were completely free of any detergent.

Preparation of affinity-purified anti-CLIC antibodies

Recombinant CLIC1 and CLIC4 were subjected to sodium dodecyl sulfate polyacrylamide gel electrophoresis and electrophoretically transferred to polyvinylidene difluoride membranes. Membrane strips containing the proteins were blocked with 5% (w/v) nonfat milk in phosphate-buffered saline (PBS), washed in PBS, and incubated overnight at 4°C with rabbit anti-CLIC antiserum raised to soluble, properly folded, full-length CLIC1 or full-length CLIC4. After extensive washing in PBS containing 0.05% (v/v) Tween-20, then PBS alone, specifically bound antibodies were eluted with 100 mM glycine-HCl (pH 2.5), immediately readjusted to a pH of 8.0 with a precalibrated amount of Tris base, and stored in small aliquots at -70°C . Western blotting with enhanced chemiluminescence detection was carried out as previously described (10). When assessed by immunoblotting against pure protein standards, the affinity-purified anti-CLIC1 and anti-CLIC4 pAbs could detect a minimum of 0.1 ng CLIC1 and 10 ng CLIC4, respec-

tively, and only showed measurable cross-reactivity when the proteins were increased to at least 1 μg . Protein concentrations were determined by absorbance measurements using calculated extinction coefficients, or by the micro Bio-Rad procedure (Pierce, Perbio Science, Cramlington, UK), using appropriate standards.

Protein incorporation into lipid monolayers

Monolayers (Langmuir-Blodgett films) were spread in a Teflon trough, as previously described (19), after the surface of the aqueous subphase had been cleaned repeatedly until the initial surface (lateral) pressure was <1 mN/m. Pressure/area isotherms after monolayer formation showed typical changes in surface pressure as the surface area was reduced, with shearing at ~ 45 mN/m. The monolayers were compressed to 20 mN/m (the lateral pressure of a typical lipid bilayer), and the surface area was then monitored under constant pressure conditions after the addition of soluble proteins directly to the subphase.

Incorporation of channels into planar lipid bilayers

Planar bilayers were prepared at room temperature ($\sim 20^\circ\text{C}$) from several different lipids, including purified soybean lecithin (Type IV, Sigma, Poole, UK), diphytanoylphosphatidylcholine, palmitoyl-oleoyl (PO) phosphatidylcholine, PO-phosphatidylethanolamine, PO-phosphatidylserine, and cholesterol (Avanti, Alabaster, AL). The lipids were suspended in *n*-decane (25 μg total lipid/ μl), and films were cast across a 0.3-mm hole in a polystyrene partition separating two solution-filled chambers, designated *cis* and *trans*. Using agar salt bridges, the *cis* chamber was voltage-clamped by an Axopatch 200-B amplifier, and the *trans* chamber was grounded, minimizing and offsetting liquid junction potentials, as described in detail previously (20). After thinning spontaneously to a capacitance of at least 250 pF, bilayers were bathed in 500 mM KCl *cis* vs. 50 mM KCl *trans* (all the solutions contained 10 mM Tris-HCl, pH 7.4 and 1 mM DTT, unless otherwise specified), and up to 25 ng/ml (~ 1 nM) CLIC1 was stirred into the *cis* chamber. Transmembrane currents normally appeared within 10 min., and were digitally recorded. Concentrated salt solutions were stirred into the relevant chamber as required, or the contents were changed by perfusion (at least 10 volumes). Unless otherwise specified, reagents were added to both chambers. Currents are labeled as positive or negative following the standard convention (i.e., positive currents represent net cation flux *cis* to *trans*).

Single channel analysis

Single-channel currents were filtered at 50 Hz (8-pole, low-pass Bessel-type response) and analyzed using pClamp8 software (Axon Instruments, Foster City, CA) and pStat (SPSS, Chicago, IL). Channel amplitudes were measured by fitting amplitude histograms to Gaussian distributions. Salt concentrations were corrected for activity using standard tables, and (relative) anion permeabilities (P) were calculated from the Nernst equation adapted for bi-ionic conditions:

$$P_{\text{anion}}/P_{\text{Cl}} = a[\text{Cl}]_{\text{cis}}/a[\text{anion}]_{\text{trans}} \times \exp(-zFEr/RT), \quad (1)$$

where a is the activity coefficient of the relevant salt, Er is the reversal or equilibrium potential, and z , F , R , and T have their usual significance. Relative anion versus cation permeabilities were calculated from the following form of the Goldman-Hodgkin-Katz voltage equation:

$$P_{\text{anion}}/P_{\text{cation}} = \{n \times \exp(Er/k) - 1\} / \{n - \exp(Er/k)\}, \quad (2)$$

where n is the *cis/trans* salt activity ratio and $k = RT/F$ (26 mV). The redox or half-cell (E_{redox} or E_{hc}) potential of the buffer pair 2GSH/GSSG (two reduced glutathione molecules equilibrated with oxidized glutathione in a

reaction involving the transfer of two protons and two electrons) was calculated from

$$E_{\text{redox}} = E^0 - RT/2F \times \ln([GSH]^2/[GSSG]) \text{ mV}, \quad (3)$$

where E^0 (−240 mV) is the standard redox potential. We took account of the experimental pH of 7.4 by including a pH-dependent correction of $(7.4 - 7.0) \times 2.3(RT/F) = -24$ mV.

RESULTS

Incorporation of CLIC1 into artificial membranes

In previous work involving the single-channel reconstitution of CLIC1 in bilayers, the membranes always contained phosphatidylcholine (PC) or phosphatidylethanolamine (PE), and sometimes both (including the PE in partially purified soybean lecithin (14)). Using these conditions as a starting point for our study, we compressed lipid monolayers to form “hemibilayers” (21) (Fig. 1 A), and confirmed, by observing membrane expansion under constant lateral pressure conditions (e.g., Fig. 1 B), that recombinant CLIC1 auto-inserted readily into membranes containing POPC or equimolar POPC and POPE, even with an intact His tag.

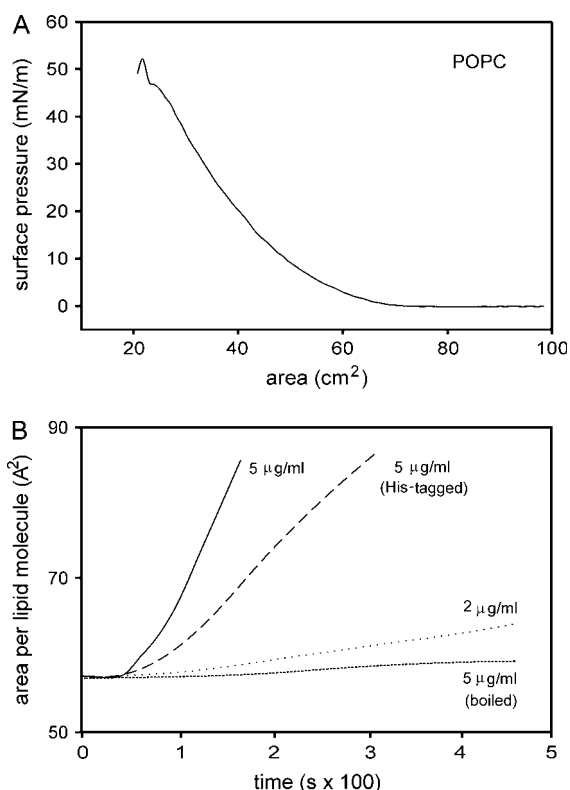


FIGURE 1 Insertion of CLIC1 into lipid monolayers. (A) Example of a pressure/area isotherm for a POPC monolayer at room temperature. The lipid was dispersed in chloroform and added carefully to the surface 20 min earlier. (B) Insertion of CLIC1 into monolayers maintained at a “bilayer-like” surface pressure of 20 mN/m. The initial area per lipid molecule (calculated from the known amount of lipid applied to the surface) was 55–60 Å², and because the amount of lipid is fixed, membrane expansion arises mainly or exclusively from protein insertion.

Surprisingly, CLIC1 failed to form well-defined ion channels in more than 20 experiments using planar bilayers containing the same lipids, with or without 1 mM DTT or 10–100 µM H₂O₂ in both chambers. This suggested that CLIC1 might require specific lipids to refold or form oligomers after membrane insertion. After extensive preliminary experiments testing a variety of lipid mixtures, we obtained highly reproducible ion channel activity in 110 of 115 experiments using POPE, POPC, and cholesterol in a molar ratio of 4:1:1 in 1 mM DTT (e.g., Fig. 2 A). We also obtained channels in the same lipid mixture in the presence of H₂O₂ from oxidized soluble CLIC1 exposed to 100 µM H₂O₂ before insertion (Fig. 2 B). This contrasted with “detergent-like” bilayer instability in other lipid mixtures, including soybean lecithin, which characteristically produced unstable anionic or cationic currents of varying amplitude. All the following data were obtained using bilayers containing POPE/POPC/cholesterol, 4:1:1 (molar), and the channels appeared to be identical with or without an intact N-terminal His tag.

Careful inspection of CLIC1 unit currents (Fig. 2 C) revealed two infrequent substates, at 45% and 22% of the main open level. As illustrated in Fig. 2, D and E, the maximum slope conductance of the main open state in a *cis:trans* gradient of 500 vs. 50 mM KCl containing 1 mM DTT in both chambers was 38 ± 3 pS (mean \pm SD, $n = 23$), and the reversal potential (E_r) of the main open state was $+6 \pm 1.1$ mV (mean \pm SD, $n = 23$ independent recordings), corresponding to a mean anion/cation permeability ratio of 1.4 (corrected for ionic activities). We noted that the conductance of channels formed from H₂O₂-oxidized CLIC1 was 24 ± 1.5 pS (mean \pm SD, $n = 10$). Channels were also obtained in the presence of 5 mM GSH in both chambers, with similar substates at 45% and 22% of the main open level. However, the apparent single-channel conductance was substantially reduced compared to DTT, to 25 ± 1.5 pS (mean \pm SD, $n = 13$).

CLIC1 channels were inhibited by IAA-94 (indanyloxy-acetic acid, Sigma, Gillingham, UK), added to the *cis* chamber, but this required very high concentrations (≥ 10 µM, data not shown), as previously observed (12,13). We therefore used affinity-purified anti-CLIC antibodies as potentially more specific functional inhibitors. Unlike our previous anti-CLIC4 antibodies (see, e.g., Proutski et al. (8)), the originating anti-CLIC1 and anti-CLIC4 antisera were generated to soluble, full-length proteins rather than N-terminally truncated proteins (see Methods). The activity of CLIC1 was completely inhibited from the *trans* side of incorporated channels by 10 µg/ml anti-CLIC1 (but not anti-CLIC4) within 30–60 s in six of six experiments, whereas prior addition of nonspecific IgG for up to 10 min had no effect (Fig. 3).

CLIC1 forms a poorly selective multi-ion pore

Fig. 4 A illustrates the current/voltage (I/V) relationship of CLIC1 in symmetric 100 mM KCl containing 1 mM DTT.

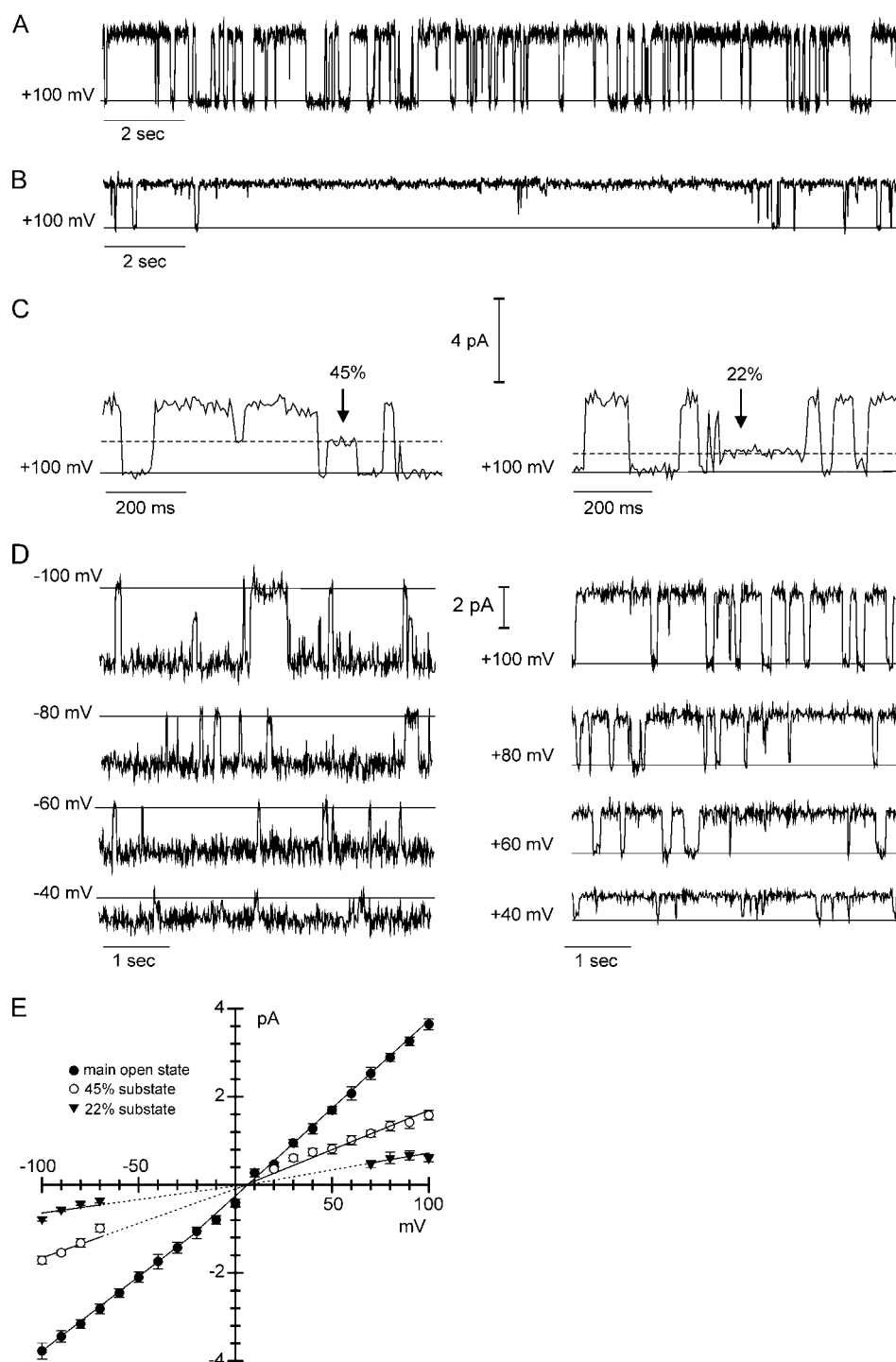


FIGURE 2 CLIC1 channels in asymmetric KCl. Single-channel recordings in 500:50 mM *cis* versus *trans* KCl containing 1 mM DTT, except where indicated. The solid lines indicate the closed current levels. (A) Contiguous 20-s recording at a holding potential (HP) of +100 mV. (B) Contiguous 20-s recording at +100 mV after exposure of CLIC1 to 100 μ M H_2O_2 before and during the recording (without DTT). (C) Selected traces on an expanded timescale showing 45% and 22% substates, HP +100 mV. (D) Single-channel currents at a range of holding potentials. (E) Corresponding current/voltage (I/V) relationships for the main open level and the two substates (shown as mean \pm SD, $n = 10$ –23). The dotted lines are extrapolations (e.g., where substate amplitudes became too small to measure).

The channel currents appeared to saturate at elevated holding potentials, but the slope conductance of the main open state was constant between +70 mV and –70 mV, with a mean value of 20.5 ± 3 pS (mean \pm SD, $n = 7$). Examples of I/V plots for full openings at relatively high and low values for [KCl] are summarized in Fig. 4 B. The conductances of the fully open state and the two substates appeared to show a nonhyperbolic dependence on KCl activity (Fig. 4 C), although

we could not obtain measurements at very low salt concentrations to confirm this behavior, and the maximum conductance of the fully open state was 57 ± 3.5 pS (mean \pm SD, $n = 7$) in symmetric 500 mM KCl (corresponding to an activity of 325 mM). However, there was a marked decline in conductance at higher salt activities (also illustrated in Fig. 4 B). The conductance of the channel was maintained at negative holding potentials, but reduced at positive potentials, in a *cis* versus

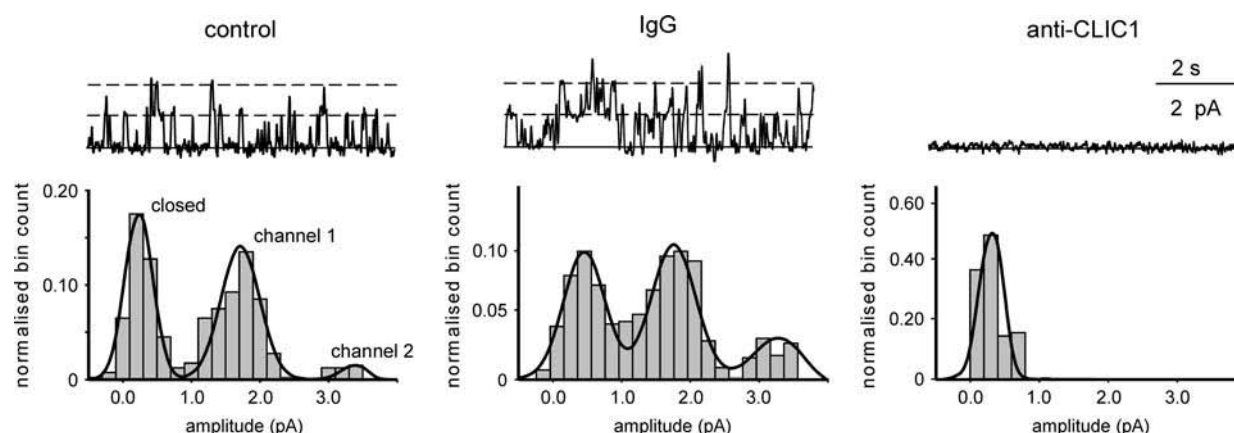


FIGURE 3 Effect of antibodies on CLIC1. Up to three recombinant CLIC1 channels in symmetrical 100 mM KCl containing 1 mM DTT. The zero-current levels are indicated by solid lines, and open channels are indicated by dashed lines. Nonspecific IgG and specific anti-CLIC1 antibodies were added where shown to a final concentration of 10 $\mu\text{g/ml}$. The amplitude histograms were constructed from long contiguous recordings lasting 60 s.

trans gradient of 500:50 mM Tris-HCl (pH 7.4) (Fig. 5 A), with a reversal potential of $+45 \pm 3.2$ mV (mean \pm SD, $n = 8$) (Fig. 5 B), reflecting a substantial increase in anion/cation permeability to 13 ± 1.0 (mean \pm SD, $n = 8$, not corrected for activities).

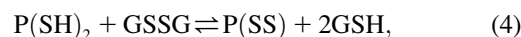
The relative permeability of a series of anions was measured under equilibrium conditions (see Methods) by perfusing the *cis* chamber with either 50 mM or 110 mM KCl (corrected for activities), followed by perfusing different potassium salts with exactly the same activity into the *trans* chamber. With (symmetrical) salt activities of 50 mM, the anion permeability sequence, calculated from the equilibrium potential as described under Methods, was I^- (1.9 ± 0.1) $>$ SCN^- (1.2 ± 0.2) \geq Cl^- (set to 1.0) \geq NO_3^{2-} (0.9 ± 0.1) \geq Br^- (0.8 ± 0.1) \geq F^- (0.7 ± 0.1). At 110 mM, the sequence became I^- (1.8 ± 0.1) $>$ F^- (1.3 ± 0.15) $=$ SCN^- (1.2 ± 0.3) $>$ Cl^- (set to 1.0) $=$ NO_3^{2-} (1.0 ± 1.0) $=$ Br^- (1 ± 1.6) (all mean \pm SD, $n = 3$ independent experiments).

CLIC1 is sensitive to redox potential

CLIC1 was reconstituted in the presence of 5 mM GSH instead of 1 mM DTT to investigate the effects of redox potential in detail, using a glutathione redox buffer system. As noted earlier, the conductance of the channels was lower in GSH (this appeared to be due to *trans* rather than *cis* GSH), although they retained the same substate pattern. They also remained open or closed for longer, often 1–10 s at our resolution (see, e.g., Fig. 6 A), too long to collect enough events for detailed gating analysis. Channels occasionally “gearshifted” into a similar gating mode in DTT, and an example of this behavior is shown later. Additions of GSSG to the *cis* chamber did not affect the single-channel conductance, but sequential additions of GSSG to the *trans* chamber decreased it from 26 ± 1.3 pS to a minimum of 2.9 ± 0.6 pS (mean \pm SD, $n = 5$) at a redox potential of -195 mV. The effect could be reversed by reverting to a

redox potential of -225 mV (5 mM GSH with 0.5 mM GSSG) in the *trans* chamber (Fig. 6 A). The substate amplitudes were also reduced, eventually becoming immeasurably small ($< \sim 0.1$ pA).

Based on a simple model for channel formation consistent with the previously proposed topology for membrane CLICs (6) (Fig. 7 A), we tested the idea that the conductance changes summarized in Fig. 6 B reflect disulphide bond formation (leading to the “closure” of an open channel) and reduction (channel opening). In that case, reactions between neighboring pairs of channel subunits can be described by the equilibrium



where “P(SS)” and “P(SH)₂” represent channel subunits with and without disulphide bonds, respectively. The kinetics are represented as intersubunit bonding because CLIC1 subunits must already be closely associated with each other in the membrane (by noncovalent interactions) to form a functional channel. The channels could undergo “graded” changes in amplitude, without resolving individual “step-like” changes between conducting (free thiol) and nonconducting (disulphide-bonded) conformations, if the disulphides are reduced relatively rapidly. This recalls the “smooth” ion channel block normally seen with (blocker) dissociation rates $> 10^5/\text{s}$, but the analogous rate in the model could of course be much slower, given the relatively heavy filtering used (22).

Employing standard mass-action treatment for the equilibrium, the disulphide and dithiol distributions can be described in terms of an equilibrium constant (K_{ox} , molar units) and the ratio $[\text{GSH}]^2/[\text{GSSG}]$:

$$K_{\text{ox}} = \{\text{P}(\text{SS})\}/\{\text{P}(\text{SH})_2\} \times \{[\text{GSH}]^2/[\text{GSSG}]\}. \quad (5)$$

The total channel protein (P_1) is the “time-averaged” sum of the reduced and oxidized protein ($[\text{P}(\text{SH})_2] + [\text{P}(\text{SS})]$), giving the proportion of reduced protein (corresponding to the relative conductance of the channel) as

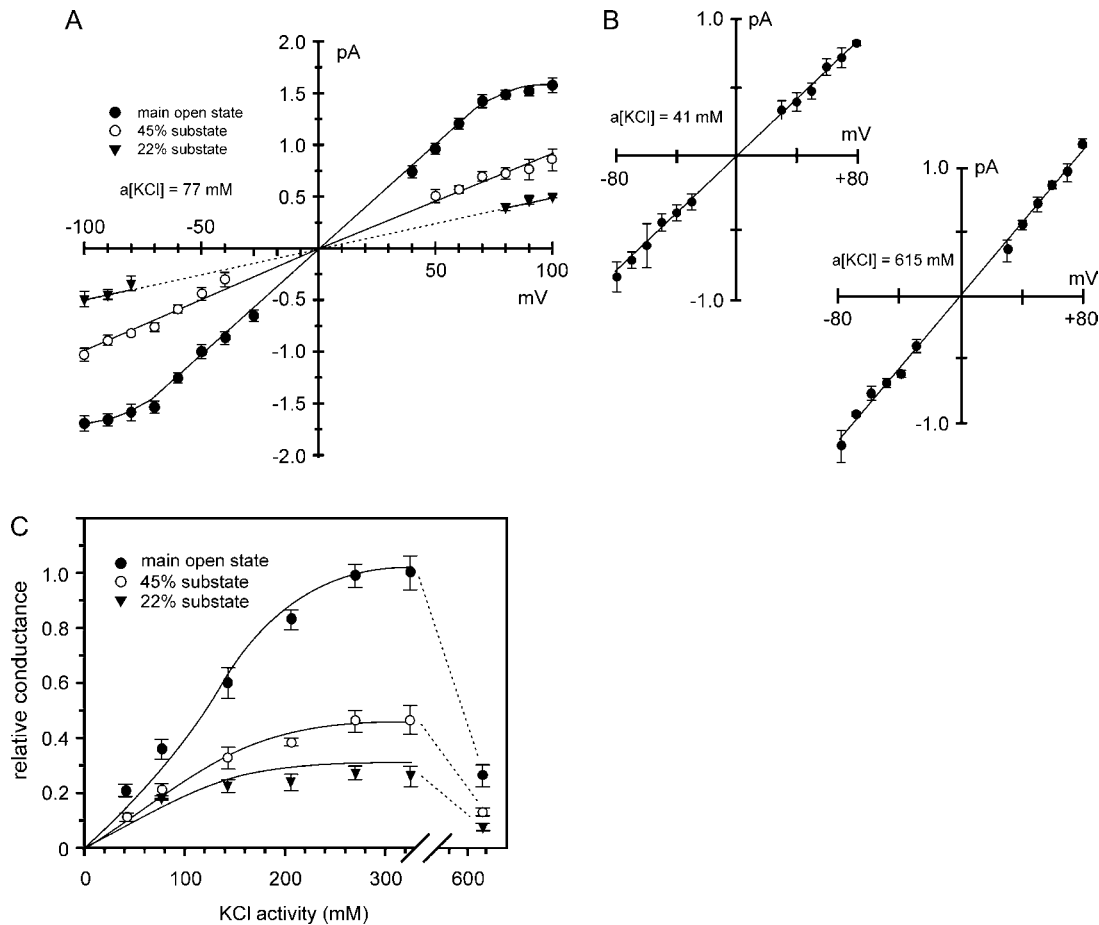


FIGURE 4 CLIC1 channels in symmetric KCl. (A) I/V relationships for each conductance level in 100 mM symmetric KCl ($a[\text{KCl}] = 77 \text{ mM}$) containing 1 mM DTT (points are shown as mean \pm SD, $n = 5-7$). The main open state is fitted to a straight line between +70 and -70 mV by linear regression ($r^2 > 0.99$). Other points are fitted by eye, with dotted lines to indicate extrapolations. (B) Examples of I/V relationships in low and high KCl activities, showing the main open state only (points are shown as mean \pm SD, $n = 3$). (C) Relative single-channel conductance-activity relationships for each conductance level in symmetric KCl solutions (points are shown as mean \pm SD, $n = 3-7$), fitted by eye. The conductance in symmetric 500 mM KCl ($a[\text{KCl}] = 325 \text{ mM}$) is set to 1.0. Note the break in the x axis between 300 and 600 mM.

$$\frac{[\text{P}(\text{SH})_2]}{[\text{P}(\text{SS})] + [\text{P}(\text{SH})_2]} = \frac{[\text{GSH}]^2/[\text{GSSG}]}{K_{\text{ox}} + [\text{GSH}]^2/[\text{GSSG}]} \quad (6)$$

Abbreviating $[\text{GSH}]^2/[\text{GSSG}]$ to $R \times [\text{GSH}]$ (where R is defined as $[\text{GSH}]/[\text{GSSG}]$),

$$\frac{[\text{P}(\text{SH})_2]}{[\text{P}_i]} = R \times [\text{GSH}] / \{K_{\text{ox}} + R \times [\text{GSH}]\} \quad (7)$$

As predicted, a plot of the (main open state) channel conductance versus the $[\text{GSH}]/[\text{GSSG}]$ ratio R , using the data summarized in Fig. 6 B, can be fitted to a rectangular hyperbola (Fig. 7 B). Additional data obtained at a GSH concentration of 2.5 mM are also plotted and fitted in the same way. The maximum conductances (at the asymptotes) coincide at $\sim 40 \text{ pS}$, similar to the conductance in fully reducing conditions (DTT). The channels cannot be fully reduced in GSH containing even minor amounts of contaminating GSSG (e.g., from autooxidation). The values of R required for half-

reduction (i.e., half the maximum channel conductance) correspond to $K_{\text{ox}}/[\text{GSH}]$, yielding $\sim 25 \text{ mM}$ for K_{ox} , irrespective of the GSH concentration.

Membrane topology of CLIC1

To test our simple model in more detail, we investigated the topology of membrane CLIC1 after preserving the N-terminal His tag. As described earlier, the tag did not affect the conductance or selectivity of the reconstituted channels. Whereas the channels remained unaffected by $50 \mu\text{M}$ *cis* NiCl_2 , channel activity disappeared in 15 of 15 experiments after stirring $50 \mu\text{M}$ NiCl_2 into the *trans* chamber (e.g., Fig. 8 A, which also provides an example of a “gearshifted” channel, as described earlier). Nontagged channels were unaffected (15 experiments). This suggested that the N-terminus of CLIC1 was on the *trans* side of the bilayer. The first cysteine residue (C24) is

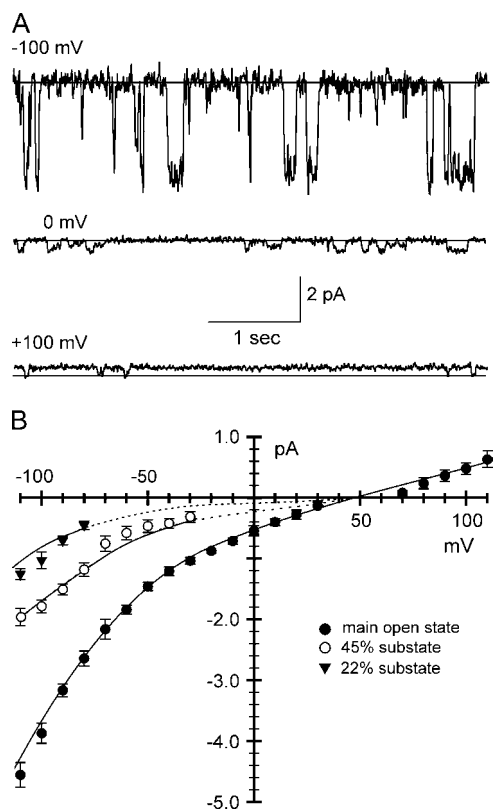


FIGURE 5 CLIC1 channels in Tris Cl. (A) Examples of single-channel currents in asymmetric Tris Cl (500:50 mM, *cis* versus *trans*) containing 1 mM DTT. The solid lines indicate the closed current levels. (B) I/V relationships for each conducting level (points are shown as mean \pm SD, $n = 5-8$), fitted by eye. The mean reversal potential is +45 mV.

located just before the start of the putative TMD (6), and is therefore also predicted to be on the *trans* side of the bilayer, close to the putative pore-forming region of (oligomeric) CLIC1 channels (Fig. 7 A). Consistent with this location, 20 μ M of the relatively bulky thiol-reactive reagent *N*-ethylmaleimide (NEM) blocked CLIC1 channels from the *trans* side in nine of nine experiments (e.g., Fig. 8 B). NEM had no effect from the *cis* side, suggesting that any cysteine residues located on this side of the bilayer are inaccessible to NEM, or they are located well away from the pore.

To further investigate the role of C24 as a potential redox- and NEM-sensitive residue on the *trans* side of the channel, it was changed to alanine. CLIC1 C24A formed channels with a reduced conductance of 14.2 ± 1.1 pS (mean \pm SD, $n = 9$) in 5 mM GSH, although the reversal potential (in 500 mM vs. 50 mM KCl) was unaltered ($+5.7 \pm 1.5$ mV, mean \pm SD, $n = 9$). Addition of Ni^{2+} to His-tagged proteins confirmed the channels remained orientated with the N-terminal tag facing the *trans* chamber. However, in nine successive experiments, the mutagenized channels, in contrast to unmodified CLIC1, were insensitive to both *trans* oxidation and *trans* NEM (e.g., Fig. 9).

DISCUSSION

Channel formation by CLIC1 is lipid-dependent

Although CLIC1 inserted readily into monolayers containing different lipids, it only assembled into specific ion channels in well-defined planar bilayers containing phosphatidylethanolamine, phosphatidylserine, and cholesterol, 4:1:1 (mol/mol). Highly specific anti-CLIC1 antibodies inhibited CLIC1 activity from the opposite side of the bilayer after adding soluble CLIC1, confirming that the protein was an essential molecular component of the channels, and that it extended through the membrane. Other lipid mixtures may prove to be equally effective, but we did not obtain consistent channel activity in any of the other lipids we tested. This suggests that although CLIC1 monomers may be able to insert into a variety of lipid membranes, native membrane CLIC1 may only assemble into functional ion channels in organelles or membrane domains containing specific lipid components. Membrane cholesterol is known to regulate pore formation by many channel-forming toxins (23), and it may be particularly relevant that in some cases (e.g., *Vibrio cholerae* cytotoxin), it may help to promote oligomerization (24).

Recent observations in microglia strongly support the idea that CLIC1 channels have an important role in cells (11), and other CLIC family members may also form ion channels by a broadly similar mechanism, although the membrane structures remain undetermined. CLIC4 (originally called p64H1), the first CLIC protein to be described, was cloned (25) in an attempt to identify the gene family encoding an intracellular IAA-94-sensitive anion channel (26) colocalized with rat brain ryanodine-sensitive Ca^{2+} -release channels (27). Rat CLIC4 is 98% identical to human CLIC4 and 67% identical to human CLIC1, and CLIC1 and CLIC4 are expressed together even in relatively primitive nervous systems (28), raising the possibility of an extended ion channel family. One reassuring characteristic of "authentic" ion channels is the accompanying evolution of regulatory mechanisms at several different levels. In this respect, many CLICs (including p64, or CLIC5B (29)) are targeted to specific organelles, where they may be localized and possibly regulated by specific protein/protein interactions (10,30). The function of membrane CLIC1 also appears to be controlled by a novel mechanism involving cysteine oxidation, and this new finding is discussed in more detail later.

Ion permeation through CLIC1

CLIC1, with six cysteine thiols, was always prepared and stored under reducing conditions, normally a stoichiometric excess of DTT. These precautions are necessary because oxidized, soluble CLIC1 forms a noncovalently linked dimer containing an intramolecular disulphide bond (16). Although the oxidized protein inserted into tip-dip bilayers to form channels of ~ 30 pS (16), compared to our finding of 24 pS for "preoxidized" CLIC1 channels, soluble CLIC1 is unlikely to exist in an oxidized form in the cytosol, which is

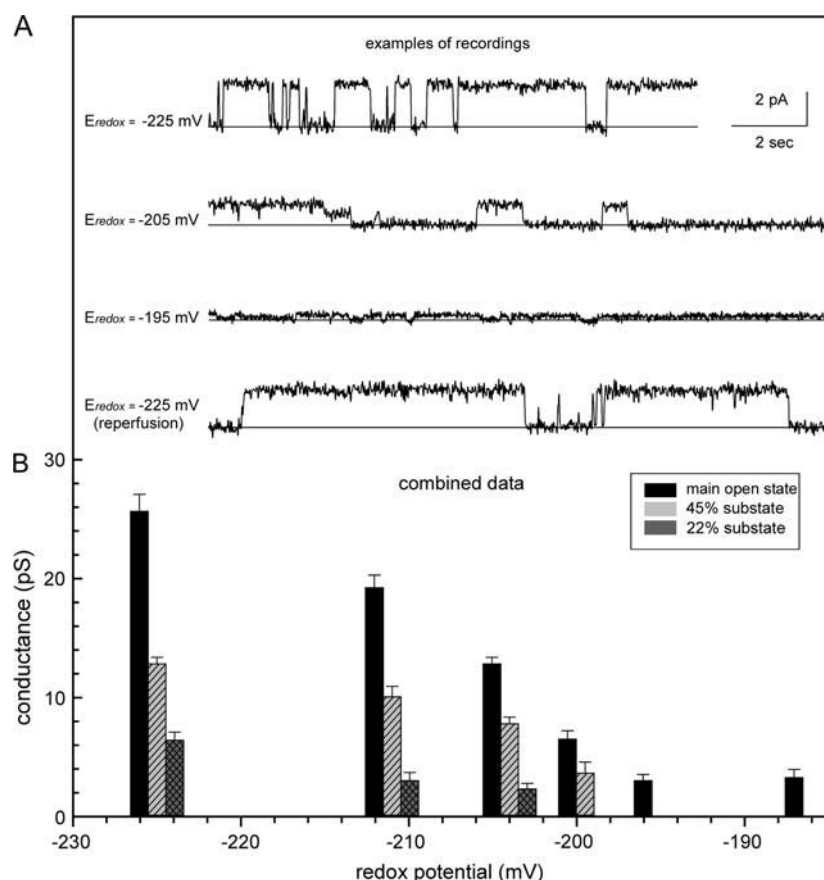


FIGURE 6 Effect of redox potential on CLIC1. (A) Selected traces in 500 vs. 50 mM KCl, HP +100 mV. The solid lines indicate the closed current levels. CLIC1 currents decrease as the redox potential in the *trans* chamber is varied from -225 mV to -195 mV using a 5 mM 2GSH/GSSG buffer system, and the effect is reversible. (B) Summary of single-channel slope conductances (shown as mean \pm SD, $n = 5$) in 2GSH/GSSG buffers providing the indicated redox potentials in the *trans* chamber. Overall, the main open state conductance decreases ~ 10 -fold with oxidation (see text).

relatively reducing and contains up to 10 mM GSH. We therefore maintained CLIC1 (or at least “cytosolic” CLIC1) in reducing conditions, and took care not to oxidize the protein before reconstituting it.

CLIC1’s substates, at 22% and 45% of the main open level, resemble two of the substates reported earlier in tip-dip bilayers (12). Similar substates in anion channels reconstituted from rat brain microsomes (26) and sheep heart inner mitochondrial membrane vesicles (20,31) were shown to be consistent with the presence of four conducting “protomers”

displaying different gating cooperativities or correlations, depending on the number of protomers open at a given instant. A similar model for CLIC1 channels requires a minimum of 16 subunits per channel (four per “protomer”, if each subunit contains just a single TMD), suggesting that cross-linked membrane complexes of functional CLIC1 channels will have a relatively large mass of at least 450,000 daltons. Some of the large conductances previously recorded for putative CLIC channels may reflect the association of groups of highly cooperative subunits into even larger structures.

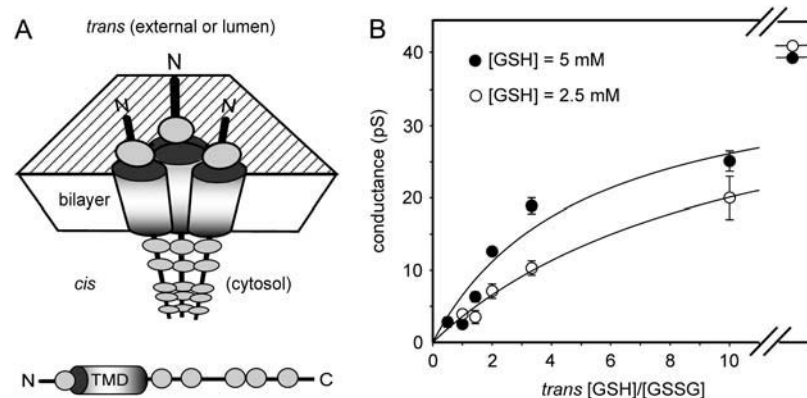


FIGURE 7 A model for CLIC1 channel assembly and regulation. (A) Cartoon view (from above and to the side) of membrane CLIC1 subunits modeled as a tetrameric ion channel, with the front subunit removed. “TMD” is a single putative transmembrane domain, and the six cysteine residues in each subunit are indicated (not to scale). Note that each membrane subunit has a single *trans* cysteine, close to the “external” pore entrance. The channels could also be modeled with more than four subunits. (B) Conductance data for the fully open state from Fig. 6B (●, mean \pm SD, $n = 5$), together with similar data from additional experiments in the presence of 2.5 mM GSH (○, mean \pm SD, $n = 3$), plotted against the $[GSH]/[GSSG]$ ratio and fitted (by least squares) to rectangular hyperbolae. The fits give maximum conductances of 39 pS and 41 pS, respectively (indicated on the asymptotes, upper right). The corresponding K_{ox} values (described in the text) are 25 mM and 26.5 mM, respectively.

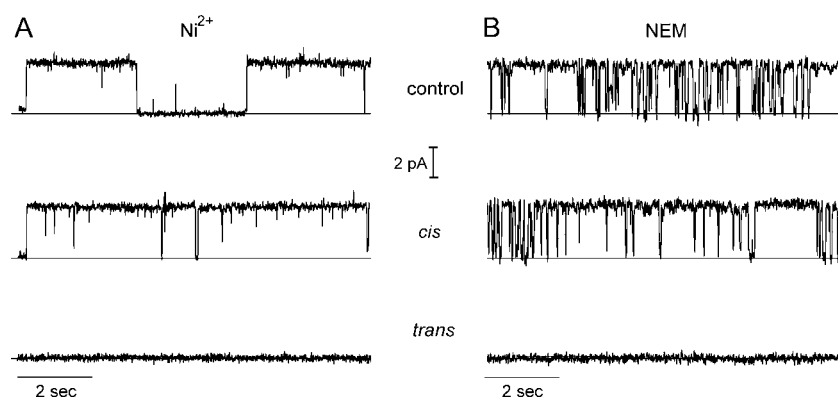


FIGURE 8 Effects of Ni^{2+} and NEM on CLIC1. (A) Addition of $50 \mu\text{M}$ Ni^{2+} to the *cis* and *trans* chambers of His-tagged channels reconstituted in 500 mM vs. 50 mM KCl in the presence of 1 mM DTT, HP +100 mV. Note the “alternative” gating mode shown in this example (see text). (B) Addition of $20 \mu\text{M}$ NEM to the *cis* and *trans* chambers of CLIC1 channels reconstituted in 500 vs. 50 mM KCl in the presence of 1 mM DTT, HP +100 mV. The DTT was removed by perfusion before making any additions. In each recording, the solid lines indicate the closed current levels.

CLIC1 is clearly a multi-ion channel (32), as demonstrated by the dependence of relative anion selectivities (as defined by reversal potentials) on ionic activity, the apparently nonhyperbolic relationship between conductance and activity, and the dramatic reduction in currents at very high activities. Although the conductances reported here are consistent with values calculated for CLIC1 in cell membranes (9), very little information is available on the selectivity of cellular CLIC1, and its relative anion versus cation selectivity has not been determined in cells. The reconstituted channels are poorly selective for anions versus cations, although their selectivity for anions improves markedly as the size of the permeant cation is increased, similar to the behavior of rat brain microsomal anion channels (26), which also showed a similar anion permeability sequence at equivalent (50 mM) activities. Overall, our results suggest that CLIC1 is a non-selective pore rather than a specific anion channel, and this obviously has significant functional implications for CLICs in cells (as well as for their nomenclature).

Redox regulation and cysteine 24

The striking *trans* redox sensitivity of CLIC1 suggested that at least one of its cysteine residues might be functionally important. Supporting this idea, *trans* NEM blocked CLIC1 (after removing free thiols from solution), but *cis* NEM had no effect. Together with a subtle but consistent voltage dependence (slightly noisier openings at negative holding potentials), this suggested the channels were inserted in a specific direction in the membrane. Because NEM actually blocked the channels, the reactive *trans* cysteine(s) were probably located in or near the pore. To help orientate CLIC1, we reconstituted the protein with an intact N-terminal His tag, knowing that membrane insertion continued under these circumstances. The tagged channels appeared to assemble normally, and their properties were indistinguishable from non-tagged proteins, except that NiCl_2 interfered with channel activity from the *trans*, but not the *cis*, chamber. Thus, both the N-terminus, and the relevant cysteine residue(s), were

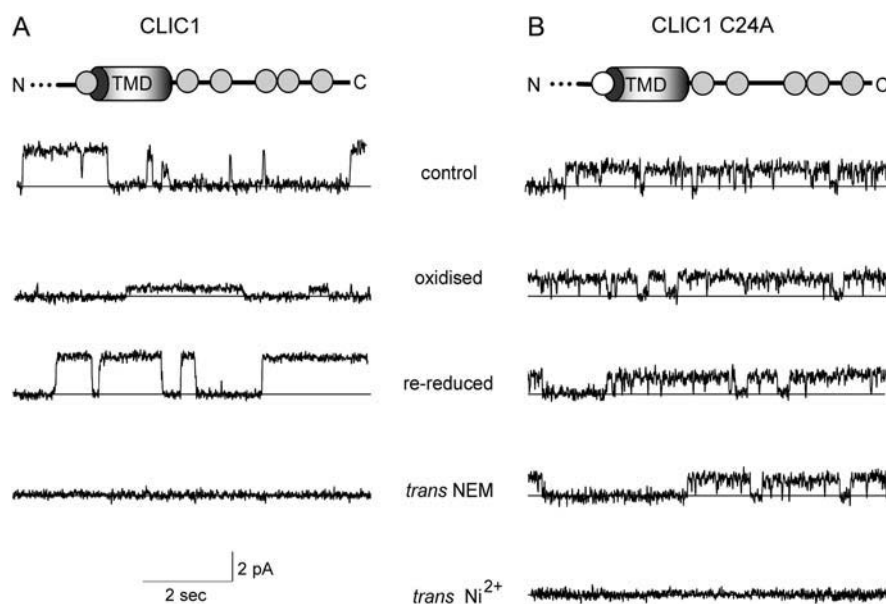


FIGURE 9 Comparison of CLIC1 and CLIC1 C24A currents. His-tagged CLIC1 and CLIC1 C24A reconstituted in 500 vs. 50 mM KCl containing 5 mM GSH and recorded at a HP of +100 mV. The cartoons (also see Fig. 7 A) summarize the locations of the cysteine residues, the position of the predicted TMD, and replacement of C24 by alanine (○). (A) CLIC1 single-channel currents responding to alterations in *trans* redox potential (−225 mV, −195 mV, and −225 mV, respectively) and block by $20 \mu\text{M}$ *trans* NEM. (B) CLIC1 C24A showing reduced overall conductance, insensitivity to the same changes in *trans* redox potential, and lack of block by $20 \mu\text{M}$ *trans* NEM. Note that $50 \mu\text{M}$ *trans* Ni^{2+} continues to inactivate the channel. In each recording, the solid lines indicate the closed current levels.

located in the *trans* chamber, corresponding to the extracellular or luminal side of the protein.

Experiments involving protease digestion (2) and antibodies targeted to the N- or C-terminus (7,8) are consistent with a single ~20-residue TMD near the N-terminus of membrane CLICs, just after the first of two cysteine-proline (CP) motifs common to many CLIC proteins, from *Xenopus* to higher organisms including mammals (28). Although the predicted TMD contains a tryptophan residue, which is atypical for a pore-lining region, this could be relevant for membrane (auto)insertion. In the *Caenorhabditis elegans* CLIC-like protein *exc-4*, substituting proline for a leucine residue in the middle of the predicted TMD, or truncating the domain, prevented membrane insertion (33). The presence of several potential cytosolic protein interaction and phosphorylation sites, from the predicted TMD all the way to the C-terminus (6), supports the idea that membrane CLICs contain just a single TMD, located near the (extracellular or *trans*) N-terminus, with the remainder of the protein in the cytosol. In this simple model for the membrane form of CLIC1, conducting channels must contain a minimum of four subunits, and in each subunit C24 is the only cysteine residue on the *trans* side of the membrane, in the CP motif just before the predicted TMD.

Implications for cellular CLIC1

Although C24 is very likely to be reduced in the cytosol, insertion of the residue into the lumen of certain intracellular organelles (e.g., the endoplasmic reticulum), or exposure to the oxidizing extracellular environment, could in principle result in disulphide bonds between neighboring subunits, if the residues approach closely enough. Our study is consistent with a simple functional model in which reversible disulphide bonds between neighboring subunits close or “block” the channel, provided the rate of reformation of free thiols is too fast to be resolved in our recordings. Oxidation would then also increase the apparent mean open (and closed) lifetimes, and although qualitatively this appeared to be the case, we could not collect enough events for statistical analysis. In a 2GSH/GSSG buffer, disulphide bond formation can be distinguished from the formation of glutathione mixed disulphides, because plots of relative reduced protein versus the [GSH]/[GSSG] ratio do not alter with [GSH] for the latter, as they do in our experiments. The model also explains the higher conductance of the channels in the presence of DTT ($E^0 = -312$ mV) compared to GSH, and the relatively low K_{ox} value (~25 mM) reflects the low stability of disulphide bonding in the protein compared to GSSG.

We tested the idea that C24 is the relevant redox- and NEM-sensitive residue in CLIC1 membrane subunits by replacing it with alanine. In the absence of structural data for the membrane proteins, we cannot of course exclude the possibility that CLIC1 C24A adopts an entirely new membrane conformation that not only relocates the original

redox- and NEM-sensitive cysteine residue(s), but also forms an ion channel (with, rather surprisingly, the same selectivity). However, the simplest way to explain why CLIC1 C24A is insensitive to *trans* oxidation and functional covalent modification by *trans* NEM is that C24 and A24 are both on the *trans* side of the pore. In this location, C24 may form conformationally important extracellular (or intraorganellar) disulphide bonds between neighboring subunits, explaining the redox-sensitivity of the channels, and its location in or near the putative pore-forming region could explain why the single-channel conductance is modified when C24 is replaced by alanine (as in this study), and possibly eliminated altogether when replaced by serine (16). Further work to support and extend this model could include recordings at much enhanced resolution, replacement of the remaining CLIC1 cysteines (other than C24), and investigation of the potential role of the neighboring residue, P25.

5-HT₃ receptor channels appear to be gated by *cis-trans* isomerization of a proline residue linking two transmembrane helices at the entrance to the transmembrane pore (34). If P25, in the well-conserved (28) CLIC1 CP motif discussed earlier, has a role in the gating of CLIC1, a constraining disulphide bond might interfere with side-chain flipping, and lock the pore closed (but not, apparently, open). In conclusion, our channel model predicts that CLIC1, even if it inserts into membranes and assembles into a channel-competent form in an appropriate lipid region, will be poorly conducting at best if its N-terminus is inserted into an oxidizing microenvironment (e.g., the endoplasmic reticulum, or possibly a patch-pipette), or if it faces the outside of the cell. However, the channel will become functionally relevant (and easier to detect) as the extracytosolic environment is made reducing. These predictions can be tested in future work involving native and overexpressed CLIC1 (and CLIC1 C24A) in cells.

H.S. was supported by a University of Edinburgh College of Medicine and Veterinary Medicine Scholarship, and by the Overseas Research Students Award Scheme.

REFERENCES

1. Valenzuela, S. M., D. K. Martin, S. B. Por, J. M. Robbins, K. Warton, M. R. Bootcov, P. R. Schofield, T. J. Campbell, and S. N. Breit. 1997. Molecular cloning and expression of a chloride ion channel of cell nuclei. *J. Biol. Chem.* 272:12575–12582.
2. Duncan, R. R., P. K. Westwood, A. Boyd, and R. H. Ashley. 1997. Rat brain p64H1, expression of a new member of the p64 chloride channel protein family in endoplasmic reticulum. *J. Biol. Chem.* 272:23880–23886.
3. Harrop, S. J., M. Z. DeMaere, W. D. Fairlie, T. Reztsova, S. M. Valenzuela, M. Mazzanti, R. Tonini, M. R. Qiu, L. Jankova, K. Warton, A. R. Bauskin, W. M. Wu, S. Pankhurst, T. J. Campbell, S. N. Breit, and P. M. Curmi. 2001. Crystal structure of a soluble form of the intracellular chloride ion channel CLIC1 (NCC27) at 1.4-Å resolution. *J. Biol. Chem.* 276:44993–45000.
4. Cromer, B. A., C. J. Morton, P. G. Board, and M. W. Parker. 2002. From glutathione transferase to pore in a CLIC. *Eur. Biophys. J.* 31: 356–364.

5. Dulhunty, A., P. Gage, S. Curtis, G. Chelvanayagam, and P. Board. 2001. The glutathione transferase structural family includes a nuclear chloride channel and a ryanodine receptor calcium release channel modulator. *J. Biol. Chem.* 276:3319–3323.
6. Ashley, R. H. 2003. Challenging accepted ion channel biology: p64 and the CLIC family of putative intracellular anion channel proteins (Review). *Mol. Membr. Biol.* 20:1–11.
7. Tonini, R., A. Ferroni, S. M. Valenzuela, K. Warton, T. J. Campbell, S. N. Breit, and M. Mazzanti. 2000. Functional characterization of the NCC27 nuclear protein in stable transfected CHO-K1 cells. *FASEB J.* 14:1171–1178.
8. Proutski, I., N. Karoulias, and R. H. Ashley. 2002. Overexpressed chloride intracellular channel protein CLIC4 (p64H1) is an essential molecular component of novel plasma membrane anion channels. *Biochem. Biophys. Res. Commun.* 297:317–322.
9. Valenzuela, S. M., M. Mazzanti, R. Tonini, M. R. Qiu, K. Warton, E. A. Musgrove, T. J. Campbell, and S. N. Breit. 2000. The nuclear chloride ion channel NCC27 is involved in regulation of the cell cycle. *J. Physiol.* 529:541–552.
10. Suginta, W., N. Karoulias, A. Aitken, and R. H. Ashley. 2001. Chloride intracellular channel protein CLIC4 (p64H1) binds directly to brain dynamin I in a complex containing actin, tubulin and 14–3–3 isoforms. *Biochem. J.* 359:55–64.
11. Novarino, G., C. Fabrizi, R. Tonini, M. A. Denti, F. Malchiodi-Albedi, G. M. Lauro, B. Sacchetti, S. Paradisi, A. Ferroni, P. M. Curmi, S. N. Breit, and M. Mazzanti. 2004. Involvement of the intracellular ion channel CLIC1 in microglia-mediated beta-amyloid-induced neurotoxicity. *J. Neurosci.* 24:5322–5330.
12. Warton, K., R. Tonini, W. D. Fairlie, J. M. Matthews, S. M. Valenzuela, M. R. Qiu, W. M. Wu, S. Pankhurst, A. R. Bauskin, S. J. Harrop, T. J. Campbell, P. M. Curmi, S. N. Breit, and M. Mazzanti. 2002. Recombinant CLIC1 (NCC27) assembles in lipid bilayers via a pH-dependent two-state process to form chloride ion channels with identical characteristics to those observed in Chinese hamster ovary cells expressing CLIC1. *J. Biol. Chem.* 277:26003–26011.
13. Tulk, B. M., P. H. Schlesinger, S. A. Kapadia, and J. C. Edwards. 2000. CLIC-1 functions as a chloride channel when expressed and purified from bacteria. *J. Biol. Chem.* 275:26986–26993.
14. Tulk, B. M., S. Kapadia, and J. C. Edwards. 2002. CLIC1 inserts from the aqueous phase into phospholipid membranes, where it functions as an anion channel. *Am. J. Physiol. Cell Physiol.* 282:C1103–C1112.
15. Dulhunty, A. F., P. Pouliquin, M. Coggan, P. W. Gage, and P. G. Board. 2005. A recently identified member of the glutathione transferase structural family modifies cardiac RyR2 substate activity, coupled gating and activation by Ca^{2+} and ATP. *Biochem. J.* 390:333–343.
16. Littler, D. R., S. J. Harrop, W. D. Fairlie, L. J. Brown, G. J. Pankhurst, S. Pankhurst, M. Z. DeMaere, T. J. Campbell, A. R. Bauskin, R. Tonini, M. Mazzanti, S. N. Breit, and P. M. Curmi. 2003. The intracellular chloride ion channel protein CLIC1 undergoes a redox-controlled structural transition. *J. Biol. Chem.* 279:9298–9305.
17. Miller, C. 1984. Ion channels in liposomes. *Annu. Rev. Physiol.* 46:549–558.
18. Jez, J. M., J. L. Ferrer, M. E. Bowman, R. A. Dixon, and J. P. Noel. 2000. Dissection of malonyl-coenzyme A decarboxylation from polyketide formation in the reaction mechanism of a plant polyketide synthase. *Biochemistry.* 39:890–902.
19. Harroun, T. A., J. P. Bradshaw, and R. H. Ashley. 2001. Inhibitors can arrest the membrane activity of human islet amyloid polypeptide independently of amyloid formation. *FEBS Lett.* 507:200–204.
20. Hayman, K. A., T. S. Spurway, and R. H. Ashley. 1993. Single anion channels reconstituted from cardiac mitoplasts. *J. Membr. Biol.* 136:181–190.
21. Brockman, H. 1999. Lipid monolayers: why use half a membrane to characterize protein-membrane interactions? *Curr. Opin. Struct. Biol.* 9:438–443.
22. Yellen, G. 1984. Ionic permeation and blockade in Ca^{2+} -activated K^{+} channels of bovine chromaffin cells. *J. Gen. Physiol.* 84:157–186.
23. Palmer, M. 2004. Cholesterol and the activity of bacterial toxins. *FEMS Microbiol. Lett.* 238:281–289.
24. Olson, R., and E. Gouaux. 2005. Crystal structure of the *Vibrio cholerae* cytolysin (VCC) pro-toxin and its assembly into a heptameric transmembrane pore. *J. Mol. Biol.* 29:997–1016.
25. Howell, S., R. R. Duncan, and R. H. Ashley. 1996. Identification and characterisation of a homologue of p64 in rat tissues. *FEBS Lett.* 390:207–210.
26. Clark, A. G., D. Murray, and R. H. Ashley. 1997. Single-channel properties of a rat brain endoplasmic reticulum anion channel. *Biophys. J.* 73:168–178.
27. Ashley, R. H. 1989. Activation and conductance properties of ryanodine-sensitive calcium channels from brain microsomal membranes incorporated into planar lipid bilayers. *J. Membr. Biol.* 111:179–189.
28. Shorning, B. Y., D. B. Wilson, R. R. Meehan, and R. H. Ashley. 2003. Molecular cloning and developmental expression of two chloride intracellular channel (CLIC) genes in *Xenopus laevis*. *Dev. Genes Evol.* 213:514–518.
29. Redhead, C., S. K. Sullivan, C. Koseki, K. Fujiwara, and J. C. Edwards. 1997. Subcellular distribution and targeting of the intracellular chloride channel p64. *Mol. Biol. Cell.* 8:691–704.
30. Shanks, R. A., M. C. Larocca, M. Berryman, J. C. Edwards, T. Urushidani, J. Navarre, and J. R. Goldenring. 2002. AKAP350 at the Golgi apparatus. II. Association of AKAP350 with a novel chloride intracellular channel (CLIC) family member. *J. Biol. Chem.* 277:40973–40980.
31. Hayman, K. A., and R. H. Ashley. 1993. Structural features of a multisubstate cardiac mitoplast anion channel: inferences from single-channel recording. *J. Membr. Biol.* 136:191–197.
32. Hille, B. 1992. *Ionic Channels of Excitable Membranes*, 2nd ed. Sinauer Associates, Sunderland, MA. 374–389.
33. Berry, K. L., H. E. Bulow, D. H. Hall, and O. Hobert. 2003. A *C. elegans* CLIC-like protein required for intracellular tube formation and maintenance. *Science.* 302:2134–2137.
34. Lummis, S. C. R., D. L. Breene, L. W. Lee, H. A. Lester, R. W. Broadhurst, and D. A. Dougherty. 2005. *Cis-trans* isomerization at a proline opens the pore of a neurotransmitter-gated ion channel. *Nature.* 438:248–252.